

Tuning the Surface Charge of 2D Oxide Nanosheets and the Bulk-Scale Production of Superlatticelike Composites

Xingke Cai,^{†,‡} Tadashi C. Ozawa,[†] Asami Funatsu,[†] Renzhi Ma,[†] Yasuo Ebina,[†] and Takayoshi Sasaki^{*,†,‡}

[†]International Center for Materials Nanoarchitectonics (WPI-MANA), National Institute for Materials Science (NIMS), Namiki 1-1, Tsukuba, Ibaraki 305-0044, Japan

[‡]Graduate School of Pure and Applied Sciences, University of Tsukuba, 1-1-1 Tennodai, Tsukuba, Ibaraki 305-8571, Japan

S Supporting Information

ABSTRACT: The surface charge of various anionic unilamellar nanosheets, such as graphene oxide (GO), $\text{Ti}_{0.87}\text{O}_2^{0.52-}$, and $\text{Ca}_2\text{Nb}_3\text{O}_{10}^-$ nanosheets, has been successfully modified to be positive by interaction with polycations while maintaining a monodispersed state. A dilute anionic nanosheet suspension was slowly added dropwise into an aqueous solution of high molecular weight polycations, which attach on the surface of the anionic nanosheets via electrostatic interaction. Surface modification and transformation to positively charged nanosheets were confirmed by various characterizations including atomic force microscopy and zeta potential measurements. Because the sizes of the polycations used are much larger than the nanosheets, the polymer chains may run off the nanosheet edges and fold to the fronts of the nanosheets, which could be a reason for the continued dispersion of the modified nanosheets in the suspension. By slowly adding a suspension of polycation-modified nanosheets and pristine anionic nanosheet dropwise into water under suitable conditions, a superlatticelike heteroassembly can be readily produced. Characterizations including transmission electron microscopy and X-ray diffraction measurements provide evidence for the formation of the alternately stacked structures. This approach enables the combination of various pairs of anionic nanosheets with different functionalities, providing a new opportunity for the creation of unique bulk-scale functional materials and their applications.

The development of various two-dimensional (2D) materials with novel functionalities has become a very hot topic.¹ The 2D structure of these unilamellar or few layered nanosheets leads to a wide range of intriguing properties. The vast majority of exfoliated nanosheets are anionic 2D materials,^{1b,2} as oxide nanosheets obtained by exfoliating layered precursors are negatively charged based on their intrinsic stoichiometry.^{1b} Other important classes of nanosheets, such as graphene oxide (GO) and MoS_2 , also have negative charges on their surfaces originating from chemical modification in the delamination process.² The charges on these nanosheets make them well dispersed in solvents, and consequently, various solution-based techniques can be used to organize them as building blocks into precisely controlled nanostructures such as nanofilms, nanocomposites, hydrogels, and so forth.^{1a-c,e,3} This approach is,

therefore, highly effective and promising to develop new functional materials and devices based on 2D materials.

Positively charged nanosheets are expected to enrich the applications of 2D materials, because there are a limited number of such cationic nanosheets. The only examples are nanosheets derived from layered double hydroxides (LDH) and related phases.^{1a,b} Recent reports demonstrate that cationic hydroxide nanosheets could be used to fabricate functional films and nanocomposites with anionic oxide nanosheets and graphene oxide (GO) via the electrostatic force between them.^{1a,b,3} The resulting materials show attractive properties, such as the highly active visible light-induced oxygen generation for hybrids of Zn–Cr LDH/titania nanosheets and the high electrochemical capacitance for the molecular-scale heteroassembly of reduced GO (rGO) and redoxable LDH, e.g., Co–Ni LDH nanosheets.^{3b,c} Although these examples show great promise for this approach, the availability of cationic nanosheets being limited to hydroxides greatly hampers their applications. Therefore, it is of great importance to develop a procedure for inverting the surface charge of anionic nanosheets.

Previous studies have reported that the surface charge of GO could be changed from negative to positive through the interaction of positively charged molecules with the oxidative functional groups on GO.⁴ Additionally, the conversion of cation-exchangeable layered hosts to anion-exchangeable ones was achieved by incorporating polycations into the interlayer space.⁵ These results strongly suggest possibilities for modifying the surface charge of a diverse range of nanosheets, including transition metal oxides, dichalcogenides, and GO, using organic polyions. A key issue is to preserve the monodispersibility of the nanosheets because the simple addition of cationic species into a colloidal suspension of the anionic nanosheets generally leads to restacking-induced flocculation.

In this study, we successfully modified the surface charge of anionic nanosheets, such as GO, $\text{Ti}_{0.87}\text{O}_2^{0.52-}$, and $\text{Ca}_2\text{Nb}_3\text{O}_{10}^-$ to be positive using the high molecular weight polyelectrolytes such as polyethylenimine (PEI) ($M_w = 7.5 \times 10^5$ g) and poly-(diallyldimethylammonium chloride) (PDDA) ($M_w = 1-2 \times 10^5$ g). In addition, by mixing anionic and polycation-modified nanosheets, such as GO and PEI-modified titania nanosheets (PEI- $\text{Ti}_{0.87}\text{O}_2^{0.52-}$), in water under appropriate conditions, their superlattice stacking was promoted.

Received: January 14, 2015

Published: February 16, 2015

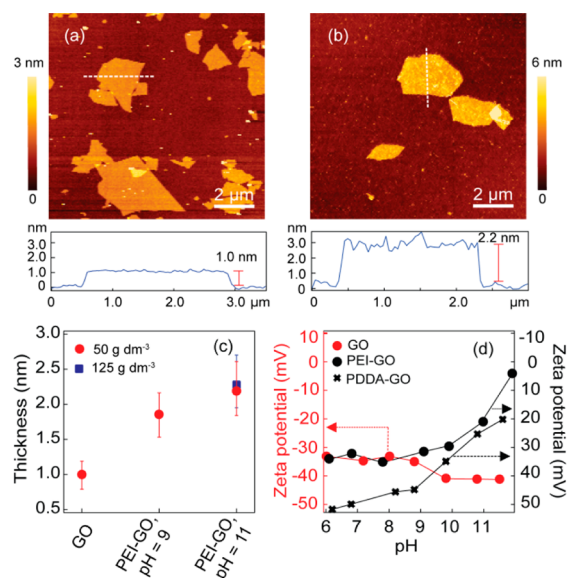


Figure 1. Typical tapping mode AFM images of (a) original GO (1.0 nm) and (b) PEI-GO (2.2 nm) deposited on a Si substrate. (c) Thickness of the original GO and final PEI-GO obtained by modifying GO with the PEI solution at different pH values (9 and 11) and concentrations (50 and 125 g dm⁻³). (d) Typical zeta potential of original GO, PEI-GO, and PDDA-GO suspensions as a function of pH value.

First, the surface of the GO was modified with the polycations. Upon dropping the GO suspension into the PEI solution ($M_w = 7.5 \times 10^5$ g), no sediment was observed in the mixed sample. Tyndall light scattering, identical to those of the original GO suspension, indicates the presence of abundant nanosheets well dispersed in the suspensions (Figure S1a,b). The color of the GO suspension changed from light yellow to dark brown upon mixing with the PEI solution (Figure 1c), which suggests some interaction between the GO and PEI. The final dark color of the PEI-modified GO (PEI-GO) suspension suggests some degree of reduction of the GO upon mixing with the PEI solution (Figure S1d). The Fourier transform infrared spectra and X-ray photoelectron spectra of the original GO and PEI-GO powder samples, recovered by high speed centrifugation and vacuum drying at room temperature, are shown in Figures S2 and S3. The data show a decrease in the intensity of the functional groups of GO, such as C=O and C–O–C, and an increase in the functional groups of PEI, such as C–N and C–C, after the modification process (Figures S2 and S3 and Table S1). These results suggest that GO and PEI are combined via the interaction between the oxidative functional groups on GO and the imine moiety of PEI. The typical atomic force microscopy (AFM) image of the PEI-GO shows the monodisperse sheets on the substrate, indicating that the nanosheets were not restacked in the suspension (Figure S4). Compared with the clean and extremely flat surface of the original GO (Figure 1a), the modified GO was somewhat rougher and thicker (Figure 1b). The thickness showed an increase from 1.0 nm for the pristine GO to 1.9 to 2.3 nm for mixed PEI solutions at pH values of 9 to 11 (Figure 1c). The increase in thickness with the pH value can be understood by the weakly acidic nature of GO; more polycations would attach on the surface of the GO because functional groups such as C–O–C tend to dissociate to produce a more negative charge, as proven by the change in the zeta potential (Figure 1d). However, the concentration of the PEI solution did not make a difference. The thickness of the PEI-GO was nearly constant even after

repeated centrifugation and washing cycles, indicating that the adsorbed PEI polycations are strongly attached onto the GO surface. Other polycations, such as PDDA ($M_w = 1-2 \times 10^5$ g) and low molecular weight PEI ($M_w = 600-800$ g), were also examined for the modification of the GO surface. The GO nanosheets were aggregated to produce a flocculate upon mixing with the low molecular weight PEI solution ($M_w = 600-800$ g, Figure S5a). A similar flocculation was previously reported when the small sized PEI molecules was added into a GO suspension.⁶ However, the GO was well dispersed in high molecular weight polyelectrolyte solutions, such as PDDA ($M_w = 1-2 \times 10^5$ g, Figure S5b) and PEI ($M_w = 7.5 \times 10^5$ g, Figure S5c). The polycations used are basically linear chain polymers with some branching. According to a rough estimate (see Supporting Information, Note S1), the length of the PEI chain is approximately 6.4 μm when the molecular weight is around 7.5×10^5 g. Note that the average lateral size of the GO is approximately 1 μm , which means that the modified GO has long polycation chains that extend over the nanosheet edge. The polycation chains in contact with the GO may neutralize the surface charges, and the chains extending outside the GO may fold to the front of the GO, providing a net positive charge on the surfaces. This configuration could prevent the approach/stacking of other modified GO. Because the PDDA used also has a high molecular weight ($M_w = 1-2 \times 10^5$ g), a similar mechanism can work to help suspend the modified GO. By contrast, the low molecular weight ($M_w = 600-800$ g) PEI is much shorter in length (5.1–6.8 nm) and is accordingly much smaller than the lateral size of the GO. Under such a situation, the GO may be able to stack together, resulting in flocculation. The zeta potential values of the PDDA-GO (PDDA: $M_w = 1-2 \times 10^5$ g) and PEI-GO (PEI: $M_w = 7.5 \times 10^5$ g) suspensions are positive, whereas the original GO is negatively charged, confirming the successful modification of the anionic GO into one with polycations on the surface (Figure 1d).

The modification of other anionic nanosheets, such as $\text{Ti}_{0.87}\text{O}_2^{0.52-}$ and $\text{Ca}_2\text{Nb}_3\text{O}_{10}^-$, was also examined using a high molecular weight polycation solution. After mixing them with the PEI ($M_w = 7.5 \times 10^5$ g) solution, the samples remained colloidal without noticeable sediment, showing Tyndall light scattering (Figure S6a–d). No change in the color or the translucent nature (Figure S6c–d) was detected, as expected, indicating the polycations are simply attached onto the anionic oxide nanosheets via electrostatic adsorption.

Here, we focus on the thickness change of $\text{Ti}_{0.87}\text{O}_2^{0.52-}$ nanosheets after the surface charge modification. A typical AFM image of the PEI- $\text{Ti}_{0.87}\text{O}_2^{0.52-}$ deposited on a substrate further suggests its good dispersion in the suspension (Figure S6e). The thickness of the PEI- $\text{Ti}_{0.87}\text{O}_2^{0.52-}$ was found to significantly increase compared with that of the pristine $\text{Ti}_{0.87}\text{O}_2^{0.52-}$ nanosheets (Figure 2a,b). The average thickness of the PEI- $\text{Ti}_{0.87}\text{O}_2^{0.52-}$ was 2.1 and 2.9 nm for the samples modified with PEI solutions having pH values of 9 and 11, respectively (Figure 2c). Similar to the case of the GO, the PEI concentrations did not influence the observed height of the modified nanosheets if their pH values were the same. The maximum increase of the thickness for the $\text{Ti}_{0.87}\text{O}_2^{0.52-}$ nanosheets (1.8 nm) was larger than that of GO (1.3 nm), which may be due to their higher surface charge density, and consequently, more polycations are adsorbed onto their surface. The thickness of the modified nanosheets remained nearly constant even when the centrifugation and washing cycles were repeated to remove the excess PEI molecules in the suspension, indicating that the adsorbed polycations were firmly

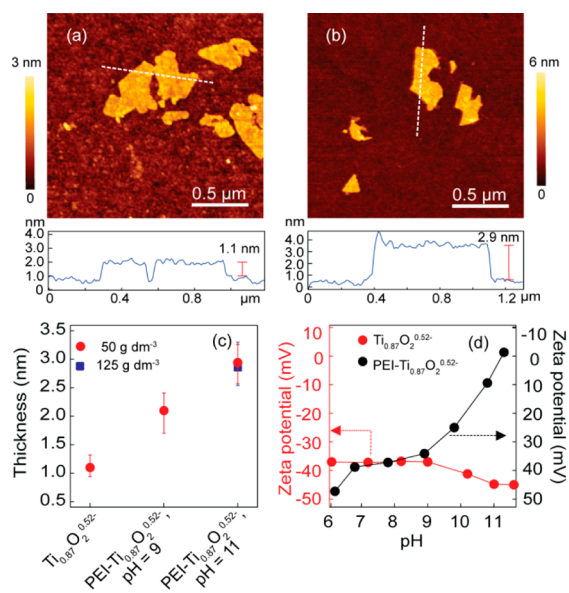


Figure 2. Typical tapping-mode AFM images of (a) original $\text{Ti}_{0.87}\text{O}_2^{0.52-}$ and (b) $\text{PEI-Ti}_{0.87}\text{O}_2^{0.52-}$. (c) Thickness of original $\text{Ti}_{0.87}\text{O}_2^{0.52-}$ and $\text{PEI-Ti}_{0.87}\text{O}_2^{0.52-}$, obtained by the treatment with the PEI solution at different pH values (9 and 11) and PEI concentration (50 and 125 g dm^{-3}). (d) Typical zeta potential of the original $\text{Ti}_{0.87}\text{O}_2^{0.52-}$ and $\text{PEI-Ti}_{0.87}\text{O}_2^{0.52-}$ as a function of pH value.

attached to the nanosheet surface. The cationic nature of the $\text{PEI-Ti}_{0.87}\text{O}_2^{0.52-}$ and $\text{PEI-Ca}_2\text{Nb}_3\text{O}_{10}^-$ was confirmed by their positive zeta potential values, as opposed to the negative values of the pristine oxide nanosheets (Figures 2d and S7).

The interaction between the colloidal suspensions of polycation-modified anionic nanosheets and anionic nanosheets is of great interest. If we use two different nanosheets, pristine and modified, we may expect the bulk-scale synthesis of superlattice-like composites based on 2D materials through flocculation. Here, we focus on modified GO and $\text{Ti}_{0.87}\text{O}_2^{0.52-}$ nanosheets, both of which are originally negatively charged and have been well studied, as an example. There are two important parameters that need to be considered for the combination, the surface area matching of the two types of nanosheets and their stability (zeta potential) in suspensions. In the restacking process of oppositely charged nanosheets, the reaction proceeds through the matching of the exact surface area of the two counterparts (1:1), whereas the total charge balance would be compensated by incorporating additional charged species such as counteranions/cations in the suspension. This mechanism has been proven in our previous study on the assembly of the cationic LDH nanosheets and anionic oxide nanosheets.^{3a,c} On the basis of the compositional and structural aspects of both nanosheets (Figure S8a–c), the weight ratio of $\text{Ti}_{0.87}\text{O}_2^{0.52-}$ to GO is estimated to be 2.8:1 to produce an equal surface area (Figure S8d). The stability of each suspension was checked by the zeta potential. As shown in Figures 1d and 2d, the zeta potential depends on the pH value. The pH values that correspond to similar absolute zeta potential values for the two suspensions were chosen for the suspensions to be mixed.

We carried out the mixing by slowly dropping the suspensions of the PEI-GO and $\text{Ti}_{0.87}\text{O}_2^{0.52-}$ nanosheets into water as a reaction medium. The suspensions with nanosheet contents corresponding to matching areas (1:1) were diluted with water into equal volume, and simultaneously injected into the water at equal dropping speeds (see Supporting Information, experimental section). In such a manner, the cationic (or modified) and

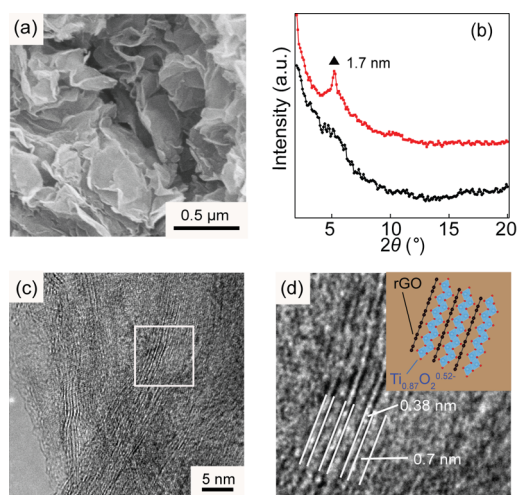


Figure 3. (a) SEM image of the sample obtained by flocculating a PEI-GO suspension (thickness: 2.2 nm) with a $\text{Ti}_{0.87}\text{O}_2^{0.52-}$ suspension (thickness: 1.1 nm). (b) XRD patterns: product in panel a (red trace), showing a peak corresponding to a basal spacing of 1.7 nm (triangle), and product obtained through the “conventional” flocculation process (black trace). (c) TEM image of the edge section of a flocculated product obtained by mixing the PEI-GO suspension with the $\text{Ti}_{0.87}\text{O}_2^{0.52-}$ suspension, followed by annealing at 300°C for 2 h. (d) Magnification of the image shown in the white box of panel c. Inset: schematic representation of the stacking nanosheets in panel d.

anionic nanosheets were fed into the reaction medium at the required proportion, under conditions in which homogeneous superlattice stacking of the oppositely charged nanosheets may proceed through their electrostatic attraction. Here, the product obtained via combining PEI-GO (thickness: 2.2 nm) and $\text{Ti}_{0.87}\text{O}_2^{0.52-}$ nanosheets (thickness: 1.1 nm) was examined as a typical example. The mixing immediately induced flocculation in the beaker. The product recovered by centrifugation and vacuum drying at room temperature was composed of lamellar materials, as shown in the scanning electron microscope (SEM) image shown in Figure 3a, indicating a face-to-face restacking of the $\text{Ti}_{0.87}\text{O}_2^{0.52-}$ and PEI-GO nanosheets. The X-ray diffraction (XRD) data showed peaks attributable to intrasheet reflections of $\text{Ti}_{0.87}\text{O}_2^{0.52-}$ and GO, indicating the coexistence of both nanosheets in the product (Figure S9). A more important feature, although broad, was detected in a low angular range (Figure 3b, red trace). The peak showing a d -spacing of $\sim 1.7 \text{ nm}$ can be identified as the second-order reflection from the alternately stacked structure of the PEI-GO and $\text{Ti}_{0.87}\text{O}_2^{0.52-}$ nanosheets. Note that the repeating dimension is expected to be 3.3 nm, as the sum of their thicknesses, which is close to double the observed d -value. Recently, we have reported the construction of superlattice-like films through layer-by-layer sequential adsorption of GO and $\text{Ti}_{0.87}\text{O}_2^{0.52-}$ nanosheets using PDDA as a counteranion.⁷ We carried out a simulation on the intensities of the basal series from the superlattice-like structure, which indicated that the second-order peak is much stronger than the first-order one. Because the films can be considered comparable to the bulk sample produced in the present study, the same interpretation is possible. In other words, the peak in Figure 3b can be taken as evidence for the alternating stacking of the modified GO and $\text{Ti}_{0.87}\text{O}_2^{0.52-}$ nanosheets.

The “conventional” procedure of the simultaneous flocculation of two different types of nanosheets involves the mixing of the nanosheet suspensions and subsequent injection of the polycat-

ion solution into the mixed suspension. Thus, it is of interest to compare the products from such a “conventional” route with the present route. The black trace in Figure 3b represents the XRD data for a sample produced by the “conventional” way; the suspensions of GO and $\text{Ti}_{0.87}\text{O}_2^{0.52-}$ nanosheets were mixed, and then PEI ($M_w = 7.5 \times 10^5$ g) solution was poured dropwise into the mixed suspension. It is clear that the sample produced by our process showed better-defined features, suggesting a better-ordered alternating stacked structure (Figure 3b, red traces). The different quality of the lamellar structure should be due to the different flocculation procedure. In the present process, two kinds of nanosheets, the modified GO and pristine $\text{Ti}_{0.87}\text{O}_2^{0.52-}$, are oppositely charged in the reaction medium, which can promote their alternate stacking. By contrast, the “conventional” process may not ideally proceed, having a chance to restack the nanosheets in a rather random way. To reveal that the present approach is applicable to various pairs of nanosheets, PEI-GO and PEI- $\text{Ti}_{0.87}\text{O}_2^{0.52-}$ were flocculated with pristine $\text{Ti}_{0.87}\text{O}_2^{0.52-}$ and GO, respectively (Figure S10). All the XRD data show peaks corresponding to basal spacings (d_i and d_i') that are half of the superlattice units (Table S2), proving that the desired alternating stacking could be achieved.

Transmission electron microscopy (TEM) images were taken to obtain atomic scale structural information, including the stacking order of the nanosheet units in the superlattices. Prior to observation, the sample made from PEI-GO and $\text{Ti}_{0.87}\text{O}_2^{0.52-}$ was annealed at 300 °C for 2 h to decompose the organic moieties to avoid contaminating the microscope. XRD data showed a greatly contracted basal peak at 1.1 nm (Figure S11). Because all the organic moieties were removed and the GO was reduced during the annealing process, the 1.1 nm may not be taken as the second-order peak of the superlattice structure, but as the first-order peak. This has been proven by high resolution TEM imaging. Lamellar lattice fringes could clearly be identified along the cross section of the annealed products (Figure 3c), and the coexistence of $\text{Ti}_{0.87}\text{O}_2^{0.52-}$ and rGO nanosheets is indicated by electron diffraction data as well as the energy dispersive X-ray analysis (Figure S12). The high resolution TEM image shows that the repeating unit of the as-prepared product is composed of two parts with different thicknesses, 0.7 and 0.4 nm, which may be attributable to $\text{Ti}_{0.87}\text{O}_2^{0.52-}$ and rGO, respectively (Figure 3d). The total thickness of 1.1 nm coincides with the XRD data shown in Figure S10d. Thus, the microscopic observation also demonstrated the superlattice stacking of the GO and $\text{Ti}_{0.87}\text{O}_2^{0.52-}$ nanosheets. The annealed products consisting of PEI- $\text{Ti}_{0.87}\text{O}_2^{0.52-}$ and GO showed a similar result (Figure S13). In addition, when the PEI- $\text{Ti}_{0.87}\text{O}_2^{0.52-}$ was flocculated with the $\text{Ca}_2\text{Nb}_3\text{O}_{10}^-$ nanosheets, the alternating stacking of them at the molecular level was also obtained (Figure S14), suggesting that the present method is widely applicable to produce a bulk heteroassembly of any two types of anionic nanosheet.

In summary, we have successfully demonstrated that the anionic nanosheets, such as GO, $\text{Ti}_{0.87}\text{O}_2^{0.52-}$, and $\text{Ca}_2\text{Nb}_3\text{O}_{10}^-$, can be modified to be positive through interaction with high molecular weight polycations, such as PEI ($M_w = 7.5 \times 10^5$ g) and PDDA ($M_w = 1-2 \times 10^5$ g) while maintaining their monodispersed unilamellar nature. The results are important because the process practically expands the nanosheet family by freely tuning the nanosheet charge. This approach may be applied to cationic nanosheets and even electrically neutral nanosheets to modify them with a desired charge. One great benefit is that the process provides a facile route to produce superlatticelike composites in bulk quantity by combining two types of

nanosheets of your choice. By slowly dropping the polycation-modified anionic nanosheets and other kinds of anionic nanosheets into water, well-structured superlattice composites consisting of two kinds of nanosheets could be spontaneously produced. Recently, the heteroassembly of multiple 2D materials has become an emerging topic because we may expect the sophisticated design of advanced functionality based on the concerted or synergistic interaction between the nanosheets. Many promising results have been reported on heteroassembled films constructed by layer-by-layer deposition processes. Although these results are intriguing and important, the layer-by-layer construction is time-consuming, and the sample quantity is rather limited. Furthermore, in many practical applications, the facile large-scale production of the material is essential. From such viewpoints, we therefore expect that the results in this work are of significant importance, providing a new process for the fundamental study and exploration of practical applications on bulk-scale superlatticelike materials based on 2D homogeneously unilamellar nanosheets.

■ ASSOCIATED CONTENT

📄 Supporting Information

Experimental details and supplementary figures. This material is available free of charge via the Internet at <http://pubs.acs.org>.

■ AUTHOR INFORMATION

Corresponding Author

*sasaki.takayoshi@nims.go.jp

Notes

The authors declare no competing financial interest.

■ ACKNOWLEDGMENTS

This work was partly supported by the World Premier International Research Center Initiative on Materials Nanoarchitectonics (WPI-MANA), MEXT, Japan.

■ REFERENCES

- (1) (a) Wang, Q.; O'Hare, D. *Chem. Rev.* **2012**, *112*, 4124–4155. (b) Ma, R.; Sasaki, T. *Adv. Mater.* **2010**, *22*, 5082–5104. (c) Wang, Q. H.; Kalantar-Zadeh, K.; Kis, A.; Coleman, J. N.; Strano, M. S. *Nat. Nanotechnol.* **2012**, *7*, 699–712. (d) Geim, A. K.; Grigorieva, I. V. *Nature* **2013**, *499*, 419–425. (e) Wang, L. Z.; Sasaki, T. *Chem. Rev.* **2014**, *114*, 9455–9486.
- (2) (a) Voiry, D.; Salehi, M.; Silva, R.; Fujita, T.; Chen, M.; Asefa, T.; Shenoy, V. B.; Eda, G.; Chhowalla, M. *Nano Lett.* **2013**, *13*, 6222–6227. (b) Yao, Y.; Lin, Z.; Li, Z.; Song, X.; Moon, K.-S.; Wong, C.-P. *J. Mater. Chem.* **2012**, *22*, 13494–13499. (c) Zhou, K.-G.; Mao, N.-N.; Wang, H.-X.; Peng, Y.; Zhang, H.-L. *Angew. Chem., Int. Ed.* **2011**, *50*, 10839–10842.
- (3) (a) Li, L.; Ma, R.; Ebina, Y.; Fukuda, K.; Takada, K.; Sasaki, T. *J. Am. Chem. Soc.* **2007**, *129*, 8000–8007. (b) Gunjakar, J. L.; Kim, T. W.; Kim, H. N.; Kim, I. Y.; Hwang, S.-J. *J. Am. Chem. Soc.* **2011**, *133*, 14998–15007. (c) Ma, R.; Liu, X.; Liang, J.; Bando, Y.; Sasaki, T. *Adv. Mater.* **2014**, *26*, 4173–4178.
- (4) (a) Yu, D.; Dai, L. *J. Phys. Chem. Lett.* **2010**, *1*, 467–470. (b) Hwang, H.; Joo, P.; Kang, M. S.; Ahn, G.; Han, J. T.; Kim, B.-S.; Cho, J. H. *ACS Nano* **2012**, *6*, 2432–2440. (c) Yang, J.; Kim, J.-W.; Shin, H. S. *Adv. Mater.* **2012**, *24*, 2299–2303.
- (5) Hata, H.; Kobayashi, Y.; Mallouk, T. E. *Chem. Mater.* **2007**, *19*, 79–87.
- (6) Tsoufis, T.; Katsaros, F.; Sideratou, Z.; Kooi, B. J.; Karakassides, M. A.; Siozios, A. *Chem.—Eur. J.* **2014**, *20*, 8129–8137.
- (7) Cai, X.; Ma, R.; Ozawa, T. C.; Sakai, N.; Funatsu, A.; Sasaki, T. *Nanoscale* **2014**, *6*, 14419–14427.